Low temperature transport and structural properties of misch-metal-filled skutterudites

J. Yang[a] and G. P. Meisner
Materials and Processes Laboratory, GM R&D Center, Warren, Michigan 48090, USA

C. J. Rawn, H. Wang, and B. C. Chakoumakos
Materials Science and Technology Division, Oak Ridge National Laboratory, Oak Ridge, Tennessee 37831, USA

J. Martin and G. S. Nolas
Department of Physics, University of South Florida, Tampa, Florida 33620, USA

B. L. Pedersen
Department of Chemistry, Aarhus University, Aarhus, Denmark

J. K. Stalick
NIST Center for Neutron Research, National Institute of Standards and Technology, Gaithersburg, Maryland 20899, USA

(Received 20 April 2007; accepted 19 August 2007; published online 16 October 2007)

Skutterudites, such as $CoSb_3$, are a promising class of thermoelectric materials, particularly when the voids in the crystal structure are filled with guest atoms. We report a comprehensive study of the effects of filling skutterudites with misch-metal (Mm), a rare-earth alloy having the naturally occurring La, Ce, Pr, and Nd composition. Our power diffraction experiments show that Mm filling causes a larger expansion and an unusual distortion of the $CoSb_3$ lattice compared with single-element-filled skutterudites. We probed the response of crystal lattice, electronic structure, and carrier and phonon scattering mechanisms to Mm filling using neutron powder diffraction, Hall effect, electrical resistivity, thermopower, and thermal conductivity measurements between 2 and 300 K on a series of $Mm_yFe_{4-x}Co_xSb_{12}$ samples. The thermoelectric properties of these Mm-filled skutterudites in this low temperature range are comparable to those of pure Ce-filled skutterudites despite the anomalous lattice expansion and distortion. We expect that these materials will have high thermoelectric figures of merit at elevated temperatures. © *2007 American Institute of Physics*. [DOI: 10.1063/1.2794716]

I. INTRODUCTION

Materials with the skutterudite structure exhibit a rich spectrum of physical behavior. This includes superconductivity, heavy fermions, magnetic ordering, hybridization gaps, non-Fermi-liquid behavior, quantum critical points, and electron-crystal-phonon-glass behavior.[1–3] In addition, filled skutterudites are technologically important because of their potential advanced thermoelectric applications for power generation.[4] The intrinsic thermoelectric performance of a material is characterized by its dimensionless figure of merit, $ZT=S^2T/\kappa\rho=S^2T/[(\kappa_L+\kappa_e)\rho]$, where T, S, κ, κ_L, κ_e, ρ are the absolute temperature, thermopower, total thermal conductivity, lattice thermal conductivity, electronic thermal conductivity, and electrical resistivity, respectively. The energy conversion efficiency of a thermoelectric power generator and the coefficient of performance of a thermoelectric cooler both increase with increasing ZT of the thermoelectric material. Therefore, a good thermoelectric material should have low κ, low ρ, and large S. The binary skutterudite compound $CoSb_3$ crystallizes in an $Im\bar{3}$ body-centered cubic structure. It is a narrow gap semiconductor with large thermopower and relatively low electrical resistance. Its thermal conductivity, however, is about 10 times higher than that of the state-of-the-art material, Bi_2Te_3, near room temperature. By filling the large interstitial voids at the $2a$ positions of the skutterudite crystal structure with rare earths, alkaline earths, or other guest atoms, the lattice thermal conductivity is drastically depressed, leading to much improved thermoelectric properties of filled skutterudites at temperatures between 600 and 800 K.[1–3] Void filling not only decreases the lattice thermal conductivity, but also plays an important role in altering the carrier concentration, carrier scattering mechanism, and hence, the electronic properties of these materials. Furthermore, as the filling fraction increases, the skutterudite crystal structure undergoes lattice expansion and distortion. Many structural changes in skutterudites can be correlated with physical properties, and are vital input for theoretical modeling, such as the *ab initio* calculations.

Misch-metal (Mm) is an alloy of rare-earth elements in their naturally occurring proportions. It is an intermediate product in the preparation of all high-purity rare-earth elements. A typical Mm composition includes predominantly Ce, La, Pr, and Nd. Most of the previous studies of filled skutterudites have been carried out using only single-element filling with a few exceptions;[1,5] recently, filled skutterudite samples were prepared using Mm,[6] but only room tempera-

[a]Electronic mail: jihui.yang@gm.com

ture thermopower data were reported. The influence of Mm filling on structural, electrical, and thermal transport properties of skutterudite $CoSb_3$ and their temperature dependences has not yet be determined and therefore is the focus of this paper.

II. EXPERIMENTAL TECHNIQUES

Four polycrystalline $Mm_yFe_{4-x}Co_xSb_{12}$ samples were synthesized from high-purity Fe, Co, and Sb. The Mm used has 52.9, 23.5, 17.4, 6.0, 0.1, and 0.1 wt % of Ce, La, Nd, Pr, Si, and Fe, respectively, as determined by electron probe microanalysis (EPMA) and wet etching chemical analysis. The samples in this study were made by a combination of arc melting, induction melting, and annealing. Stoichiometric amounts of Mm, Fe, and Co were arc melted in a Zr-gettered argon arc furnace to form Mm-Fe-Co ingots. The ingots were then loaded with the appropriate Sb amounts into boron nitride crucibles and induction melted at approximately 1350 °C for 1 m under argon to form $Mm_yFe_{4-x}Co_xSb_{12}$. The samples were crushed into powders and cold-pressed at room temperature into pellets. The pellets were then annealed at 700 °C for 1 week in sealed quartz tubes under argon. Finally, all annealed samples were crushed into powders again and then hot-pressed at 600 °C and 400 MPa under vacuum into high-density samples. X-ray powder diffraction was performed on a Philips diffractometer using Cu $K\alpha$ radiation, and lattice parameters were refined using the Rietveld method. Chemical compositions were determined by EPMA averaged over 12 randomly selected locations.

Two additional 10 g samples were synthesized using the same synthesis method (without hot pressing) for neutron powder diffraction measurements which were carried out in the temperature range from 10 to 300 K. X-ray powder diffraction was also performed for these two samples on a PANalytical X'Pert Pro multipurpose diffractometer (MPD) using Cu $K\alpha$ radiation, and lattice parameters were refined using the Rietveld method. Rietveld refinements were performed using the EXPGUI graphical user interface[7] for the General Structure Analysis System (GSAS).[8] Data were collected at the NIST Center for Neutron Research (NRCN) on the BT-1 high-resolution powder diffractometer. The instrument has 32 ^{3}He-filled detectors and was configured with a Cu (311) monochromator using a take-off angle of 90°, resulting in a wavelength of 1.5403 Å. The powder samples were contained in V cans that were placed in closed-cycle He refrigerators with two temperature sensors, one to control the temperature, and another one located at a different position for comparison. Data were collected on both samples at 10, 50, 100, 150, 200, 250, and 300 K. The data were analyzed using the Rietveld method using the neutron scattering lengths reported by Sears[9] for lanthanides, Fe, Co, and Sb. The neutron scattering lengths for the Mm sites in both samples were the weighted averages based on the results of EMPA elemental analysis for the Ce, La, Nd, and Pr contents. For the $Mm_{0.82}Fe_{3.51}Co_{0.49}Sb_{11.99}$ and $Mm_{0.88}Fe_4Sb_{12.06}$ samples the average neutron scattering length was calculated to be 5.07 and 5.44 fm, respectively. Refined structural parameters including the unit cell length, atomic displacement parameters, and positional parameter for Sb were determined, and site occupancy factors (sof) for the Mm site and the Fe/Co site.

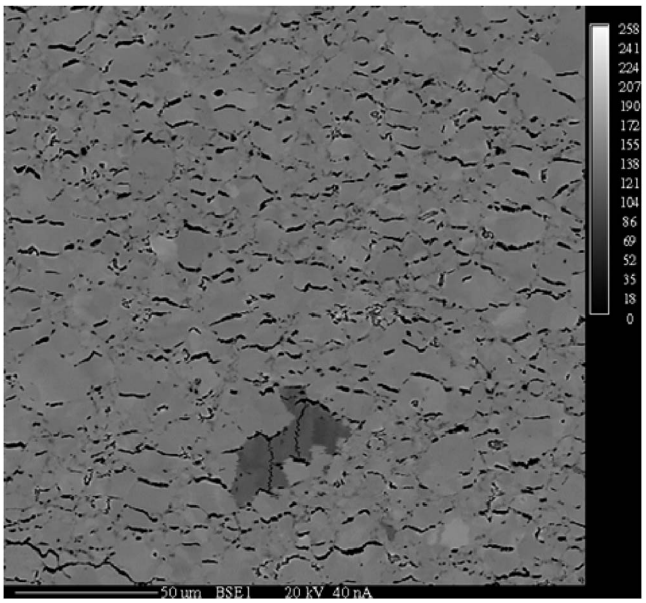

FIG. 1. Backscattered electron (BSE) image of $Mm_{0.55}Fe_{2.44}Co_{1.56}Sb_{11.96}$ focused near a secondary phase. The total amount of secondary phases is estimated to be less than 1 vol %.

Electrical resistivity (ρ), thermopower (S), and thermal conductivity (κ) measurements were made in a Quantum Design physical property measurement system (PPMS) between 2 and 300 K on $3\times3\times10$ mm^3 samples cut by a diamond saw. These measurements were done in a four-probe configuration using the continuous mode of PPMS. The accuracy of our PPMS ρ, S, and κ data are 15%, 5%, and 10%, respectively. The Hall effect and electrical resistivity were measured using a Linear Research ac bridge with 16 Hz excitation in a superconducting magnet cryostat capable of fields up to 5 T on $0.5\times1.5\times5.5$ mm^3 samples cut from the same ingots. For Hall effect measurements, data were collected in both positive and negative fields to eliminate any electrical contact misalignment effects. The accuracy of ρ and carrier concentration p data is estimated to be 5% and 10%, respectively, in the cryostat measurements.

III. RESULTS AND DISCUSSION

A. Chemical and structural properties

Our EPMA results show that all samples are close to phase pure with the exception of trace amounts of Sb, $FeSb_2$ and $MmSb_2$ ($\leq$1 vol %). The relative concentrations of rare earths in Mm-filled samples are the same as those in the starting Mm alloy. Figure 1 shows a backscattered electron image of $Mm_{0.55}Fe_{2.44}Co_{1.56}Sb_{11.96}$ with the dark region being a secondary phase. Table I lists the nominal composition, the actual composition, and room temperature lattice parameter of $Mm_yFe_{4-x}Co_xSb_{12}$ samples. The two samples labeled with asterisks were made for neutron powder diffraction only, and we did not measure their transport properties. The nominal, or target, compositions were selected based on the maximum Ce filling fractions in the $CoSb_3$ crystal lattice.[10]

TABLE I. Nominal composition, actual composition; and room temperature lattice parameter, total thermal conductivity κ, thermopower S, electrical resistivity r, and hole concentration p of $Mm_yFe_{4-x}Co_xSb_{12}$. The uncertainties of various data are listed in the text. Samples labeled with asterisks were made for neutron powder diffraction measurements only.

Nominal composition	Actual composition	Room temperature lattice parameter (Å)	κ (W/mK)	S (μV/K)	ρ ($\mu\Omega$ cm)	p (10^{21} cm^{-3})
$Mm_{0.71}Fe_{2.5}Co_{1.5}Sb_{12}$	$Mm_{0.55}Fe_{2.44}Co_{1.56}Sb_{11.96}$	9.104(5)	2.1	99	9.5	1.1
$Mm_{0.82}Fe_3CoSb_{12}$	$Mm_{0.65}Fe_{2.92}Co_{1.08}Sb_{11.98}$	9.114(3)	2.5	75	6.4	0.6
$Mm_{0.93}Fe_{3.5}Co_{0.5}Sb_{12}$	$Mm_{0.72}Fe_{3.43}Co_{0.57}Sb_{11.97}$	9.128(3)	2.5	81	5.2	1.8
$MmFe_4Sb_{12}$	$Mm_{0.82}Fe_4Sb_{11.96}$	9.142(1)	2.8	72	4.3	3.6
$Mm_{0.93}Fe_{3.5}Co_{0.5}Sb_{12}$*	$Mm_{0.82}Fe_{3.51}Co_{0.49}Sb_{11.99}$	9.1294(2)				
$MmFe_4Sb_{12}$*	$Mm_{0.88}Fe_4Sb_{12.06}$	9.1433(2)				

The actual Mm filling fractions (y) in all samples are less than the corresponding nominal values due to Mm vapor losses during arc melting and induction melting. In the case of the two samples made for neutron diffraction, additional Mm was added to the starting materials and resulted in larger y values, closer to the nominal composition. Room temperature lattice parameters are plotted in Fig. 2 versus y. The lattice parameter in $CoSb_3$ increases not only by increasing rare-earth filling (y), but also replacing Co with Fe. The lattice parameter difference between the two samples with $y=0.82$ (but with different x values) can be accounted for, within the acceptable standard errors, if we use the same rate of lattice parameter increase as a function of increasing Fe concentration observed for $Co_{1-x}Fe_xSb_3$.[11] These results indicate that Mm filling expands the skutterudite lattice more rapidly than La and Ce filling does at the same filling fraction. This is surprising because one would expect the lattice parameters of Mm-filled skutterudites to be linear combinations of those of Ce-, La-, Nd-, and Pr-filled skutterudites, and not to exceed those of La-filled skutterudites (the largest),[12] with the same filling fractions. In addition, we observe that the y coordinate of Sb in these Mm-filled skutterudites (see Table II) behaves differently than the general trend suggested by Chakoumakos and Sales[13] for single-rare-earth-filled skutterudites. The latter have nearly square Sb rings ($y+z\approx 1/2$) in the crystal structure near 100% filling fraction, whereas the Mm-filled samples have slightly rectangular Sb rings (3% distortion). We do not know the exact mechanism that causes the unusually large cell volume and lattice distortion, but speculate that it arises from the additional lattice strain induced by the mixture of rare earths with different sizes and bonding schemes with their neighboring atoms.

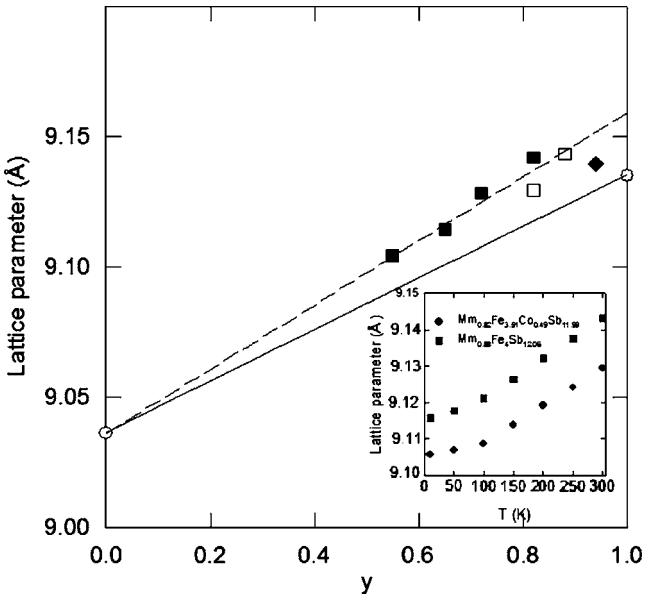

FIG. 2. Lattice parameter measured at room temperature vs Mm filling fraction y for $Mm_yFe_{4-x}Co_xSb_{12}$. Filled and unfilled squares represent data determined by x-ray and neutron powder diffractions, respectively. Lattice parameters of $CoSb_3$ and $CeFe_4Sb_{12}$ (unfilled circles) are also plotted for comparison. The filled diamond represents data for $LaFe_4Sb_{12}$ (Ref. 12). The dashed and solid lines represent the linear variation of lattice parameter for $Mm_yFe_{4-x}Co_xSb_{12}$ and for $Ce_yFe_{4-x}Co_xSb_{12}$, respectively (Ref. 10). Inset: lattice parameters refined from neutron power diffraction data as a function of temperature between 10 and 300 K of $Mm_{0.82}Fe_{3.51}Co_{0.49}Sb_{11.99}$ and $Mm_{0.88}Fe_4Sb_{12.06}$.

The inset in Fig. 2 shows the temperature dependence of the lattice parameter of $Mm_{0.82}Fe_{3.51}Co_{0.49}Sb_{11.99}$ and $Mm_{0.88}Fe_4Sb_{12.06}$ between 10 and 300 K determined from neutron diffraction data. The lattice parameters of these two samples increase by 0.26% and 0.30%, respectively, upon heating from 10 to 300 K, and the linear thermal expansion coefficients at room temperature are 1.135×10^{-5} K^{-1} and 1.135×10^{-5} K^{-1}, respectively. The crystal structure was modeled using the cubic crystal system and space group $Im\bar{3}$. The starting coordinates and lattice parameter for modeling the crystal structure were taken from Kaiser *et al.*[14] Twenty-six and 25 variables were used to fit the neutron powder diffraction data for the two samples, respectively. A shifted Chebyshev polynomial with 12 terms was used to fit the background, four profile parameters were used to fit the peak

TABLE II. Crystal structure refinement data of neutron powder diffraction for $Mm_{0.82}Fe_{3.51}Co_{0.49}Sb_{11.99}$ and $Mm_{0.88}Fe_4Sb_{12.06}$ at 300 K, based on the skutterudite crystal structure, space group $Im\bar{3}$, with Mm, Fe/Co, and Sb occupying the 2a 0, 0, 0; 8c 1/4, 1/4, 1/4; and 24g 0, y,z sites, respectively.

Sample	$Mm_{0.82}Fe_{3.51}Co_{0.49}Sb_{11.99}$	$Mm_{0.88}Fe_4Sb_{12.06}$
Lattice parameter (Å)	9.1294(2)	9.1433(2)
U_{iso} (Mm) (Å^2)	0.021(1)	0.023(1)
U_{iso} (Fe/Co) (Å^2)	0.0067(2)	0.0056(2)
U_{iso} (Sb) (Å^2)	0.0078(2)	0.0072(2)
y (Sb)	0.3357(2)	0.3362(2)
z (Sb)	0.1599(1)	0.1603(2)
Variable	26	25
χ^2	1.127	1.331

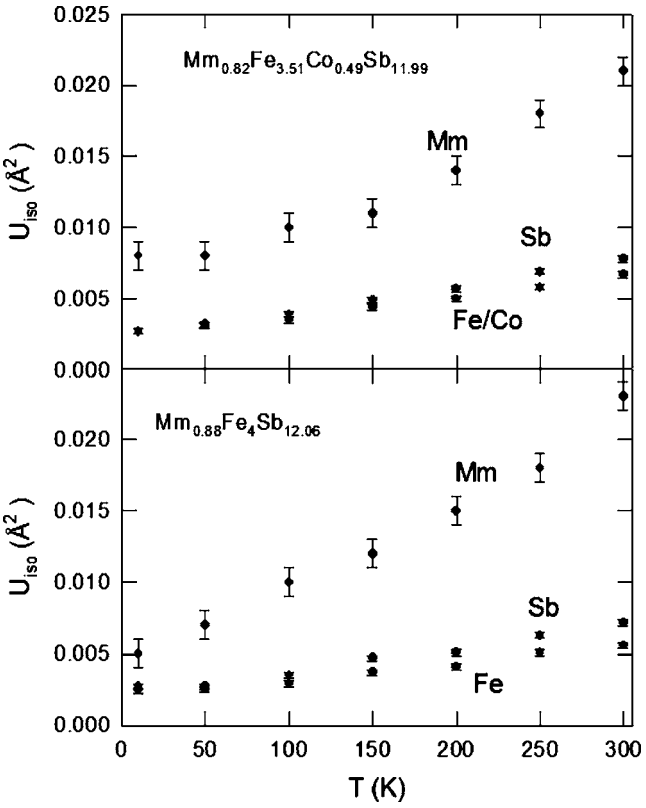

FIG. 3. Isotropic atomic displacement parameter of Mm, Fe/Co, and Sb sites vs temperature between 10 and 300 K for $Mm_{0.82}Fe_{3.51}Co_{0.49}Sb_{11.99}$ and $Mm_{0.88}Fe_4Sb_{12.06}$.

shape, and a 2θ zero offset and a scaling factor were included for a total of 18 variables for each case. Atomic variables include the lattice parameter, the y and z atomic coordinates for the Sb atom, and the isotropic atomic displacement parameters (ADP) for the three sites, and the site occupancy factor for the Mm site. The additional variable for $Mm_{0.82}Fe_{3.51}Co_{0.49}Sb_{11.99}$ was the site occupancy factor of the Fe/Co site. In this site the total occupancy was constrained to 100% with 12.25% Co and 87.75% Fe, and the atomic displacement parameters were constrained to be equal. For both samples the refined amount of Mm was higher than that determined from the EMPA analysis, i.e., $Mm_{0.96}Fe_4Sb_{12}$ compared to $Mm_{0.88}Fe_4Sb_{12.06}$ and $Mm_{0.92}Fe_{3.56}Co_{0.44}Sb_{12}$ compared to $Mm_{0.82}Fe_{3.51}Co_{0.49}Sb_{11.99}$. This suggests that the average scattering factors are slightly different than those used and could have an effect on the results of the refined ADPs since it is highly correlated with the sof. The neutron power diffraction structure refinement results are listed in Table II.

The isotropic atomic displacement parameters U_{iso} for various sites, also determined by neutron powder diffraction, are plotted in Fig. 3 as a function of temperature between 10 and 300 K. U_{iso} represents the mean square displacement amplitude of an atom averaged over all directions. The temperature-independent part of U_{iso} is attributed to static disorder, whereas the temperature-dependent part arises from dynamic disorder—vibration of an atom around its equilibrium position.[15] For both samples in Fig. 3, the Mm sites have much larger U_{iso} than the Fe/Co and Sb sites. If we assume that the rare-earth atoms on the Mm sites rattle as quantized Einstein oscillators, U_{iso} can be written as

$$U_{iso} = \frac{\hbar}{2m\omega_0}\coth\left(\frac{\hbar\omega_0}{2k_BT}\right), \quad (1)$$

where $\hbar$ is the reduced Planck constant, m the atomic mass, ω_0 the resonant frequency, and k_B the Boltzmann constant. At high temperatures where $\hbar\omega_0 \ll 2k_BT$, Eq. (1) can be simplified as $U_{iso}=k_BT/m\omega_0^2$. From the linear slopes of U_{iso} versus T between 150 and 300 K in Fig. 3, we can estimate values of ω_0, which represents the average frequency at which various rare-earth atoms rattle inside their interstitial voids (the Mm sites). The average Einstein temperature is then determined by $\theta_E^{ave}=\hbar\omega_0/k_B$, and it is 72.5 K for $Mm_{0.82}Fe_{3.51}Co_{0.49}Sb_{11.99}$ and 70.5 K for $Mm_{0.88}Fe_4Sb_{12.06}$. The Einstein temperatures for La-, Ce-, Eu-, and Yb-filled skutterudites are 80 K (from inelastic neutron scattering), 78 K (from neutron powder diffraction), 83 K (from inelastic nuclear scattering), and 65 K (from neutron powder diffraction), respectively.[16–18] These results suggest that the average frequency at which rare-earth atoms rattle on the Mm sites of these Mm-filled skutterudites is comparable to those rattling frequencies observed individually for Ce, La, and Yb. This further implies that using multiple rare-earth fillers in an effort to scatter a broader range of lattice phonons and thereby achieve lower lattice thermal conductivity is ineffective. The low temperature intercepts of U_{iso} with the vertical axis in Fig. 3 represent a combination of zero-point vibration and static disorder at the corresponding crystallographic sites. The zero-point vibration is inversely proportional to the mass of the atom, so we would expect that contribution to be Mm < Sb < Fe/Co. This implies that there is some positional disorder associated with the Sb site and more so with the filling atom site. According to the data shown in Fig. 3, the static disorder at Fe/Co sites is almost identical for $Mm_{0.82}Fe_{3.51}Co_{0.49}Sb_{11.99}$ and $Mm_{0.88}Fe_4Sb_{12.06}$. This is because the mass and size differences between Fe and Co are small (5% and 10%, respectively), and therefore replacing Co with Fe leads to negligible lattice static disorder. A larger amount of static disorder on the Mm sites is observed for $Mm_{0.82}Fe_{3.51}Co_{0.49}Sb_{11.99}$. The ratios of the low temperature U_{iso} intercepts on the Mm sites for the two samples are roughly proportional to their corresponding $y(1-y)$ values, validating that the static lattice disorder on the Mm sites arises between Mm_y and $\square_{1-y}$, where $\square$ represents a crystallographic void.[10,19]

B. Electrical resistivity, thermopower, and carrier concentration

The electrical resistivity and thermopower for the first four samples listed in Table I are plotted in Figs. 4 and 5 as a function of temperature between 2 and 300 K. Except for $Mm_{0.55}Fe_{2.44}Co_{1.56}Sb_{11.96}$ at low temperatures ($T<150$ K), ρ increases monotonically as T increases for all samples. Room temperature ρ values are all less than 1 mΩ cm, and S values are between 77 and 100 μV/K. These values of ρ and S are indicative of heavily doped semiconductors and are comparable to those found in single-element-filled

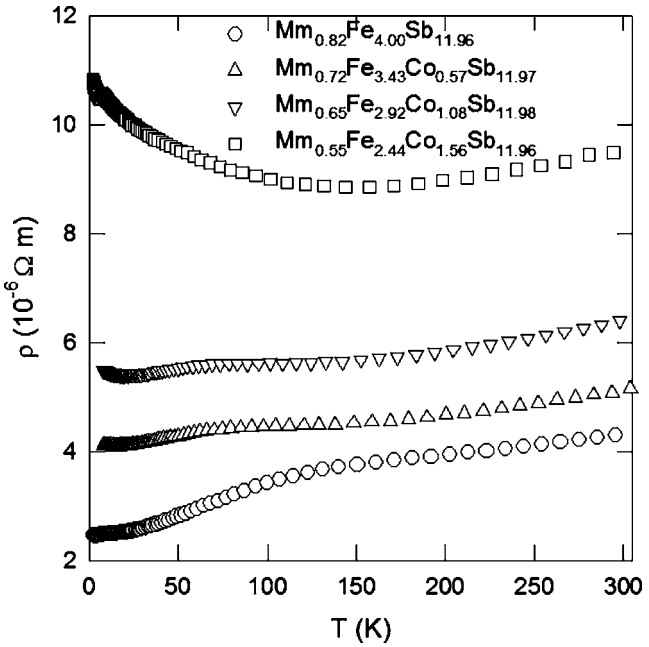

FIG. 4. Electrical resistivity vs temperature between 2 and 300 K for $Mm_yFe_{4-x}Co_xSb_{12}$.

skutterudites.[1–3] The carrier concentrations p are plotted in Fig. 6(a) between 2 and 300 K, showing that these samples are all p-type and that the hole concentrations are between 3×10^{20} and 3×10^{21} cm^{-3}. The hole mobilities in the same temperature range are shown in Fig. 6(b). The $\mu_H \propto T^{-3/2}$ behavior expected from hole-acoustic phonon scattering is illustrated in Fig. 6(b) by a solid line near room temperature. The data shown in Fig. 6(b) imply that holes are less likely to be scattered by only one mechanism. If we assume a mixed ionized impurity and acoustic phonon scattering for holes near room temperature, for a single parabolic band, S and p are given by

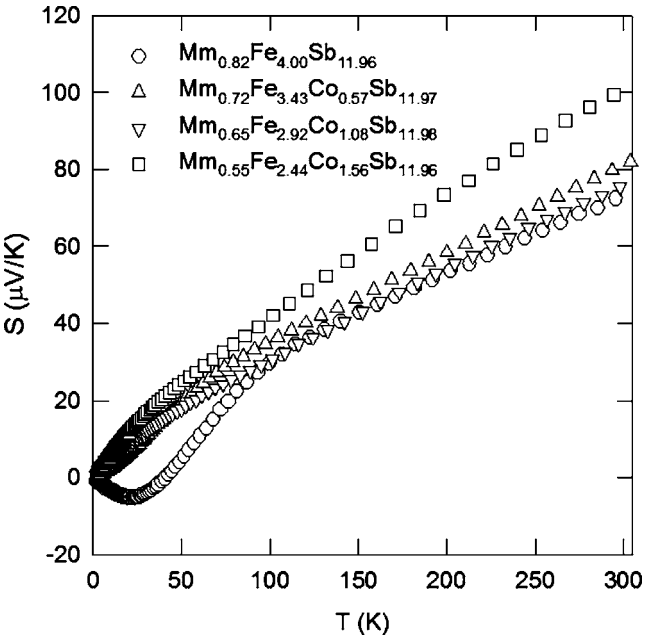

FIG. 5. Thermopower vs temperature between 2 and 300 K for $Mm_yFe_{4-x}Co_xSb_{12}$.

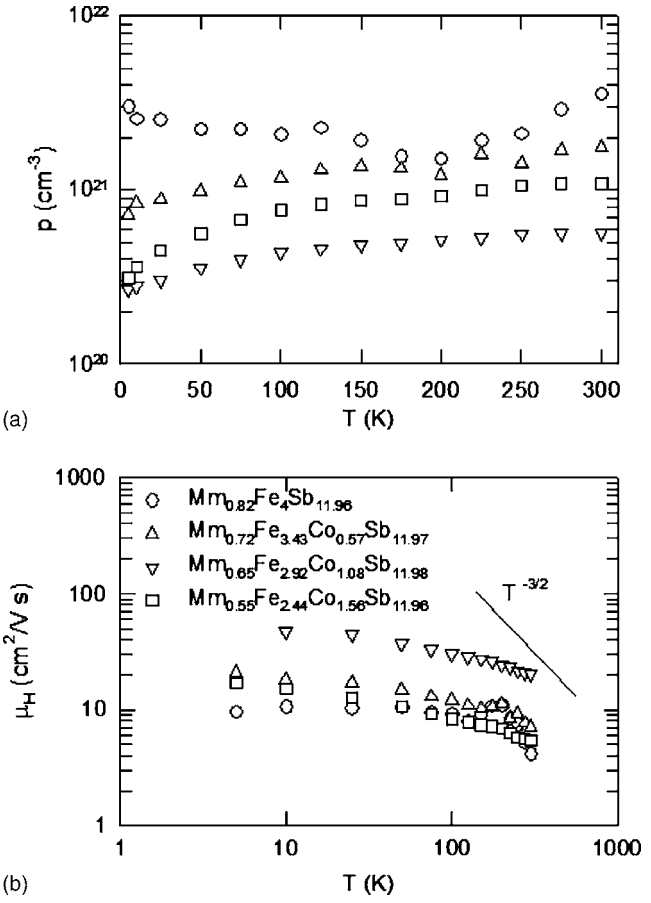

FIG. 6. (a) Hole concentration and (b) hole mobility vs temperature between 2 and 300 K for $Mm_yFe_{4-x}Co_xSb_{12}$.

$$S = \frac{k_B}{e}\left(\frac{(2+r)F_{1+r}(\eta)}{(1+r)F_r(\eta)} - \eta\right), \tag{2}$$

$$p = \sqrt{\frac{2}{\pi}}\left[\frac{m^* k_B T}{\hbar^2}\right]^{3/2} F_{1/2}(\eta), \tag{3}$$

where r is the exponent of the energy dependence of the hole mean-free-path, m^* the hole effective mass, e the electron charge, $\eta = E_F/k_BT$ the reduced Fermi energy, E_F the Fermi energy, and F_x the Fermi integral of order x. For holes scattered by ionized impurities and acoustic phonons, $r=2$ and 0, respectively. We use the intermediate value $r=1$ for mixed scattering.[20] Room temperature S and p data yield m^* between $1.3m_e$ and $4.5m_e$, where m_e is the free electron mass. These effective mass values are much larger than that reported for near the top of the $CoSb_3$ valence band ($0.175m_e$).[21] This indicates that $CoSb_3$ valence band curvature changes significantly from the top toward deep into the band. Because of these heavy hole masses, the heavily doped p-type skutterudites sustain relative large power factor (S^2/ρ) values. Similar results have been reported in Ce-filled and other filled skutterudites.[1,10,22] Recently, spin-fluctuation scattering has been proposed to be a possible carrier scattering mechanism in filled skutterudites.[23,24] Because of the low spin-fluctuation temperatures ~50 K,[23,24] we do not expect it to be significant near room temperature. The room temperature power factor versus hole concentration is shown in

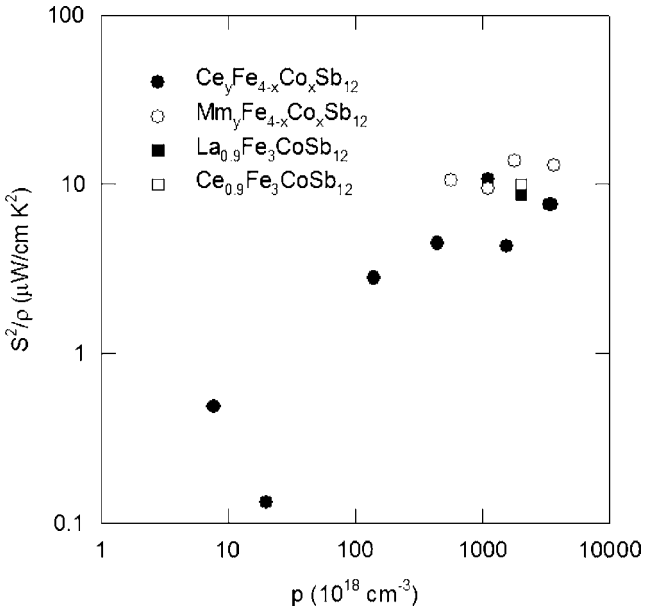

FIG. 7. Power factor vs hole concentration for $Mm_yFe_{4-x}Co_xSb_{12}$, $Ce_yFe_{4-x}Co_xSb_{12}$, $La_{0.9}Fe_3CoSb_{12}$, and $Ce_{0.9}Fe_3CoSb_{12}$ (Refs. 10 and 22).

Fig. 7, and some Ce- and La-filled skutterudite data are included for comparison. The Mm-, Ce-, and La-filled skutterudites have comparable power factor values near $p=1\times10^{21}$ cm^{-3}.

C. Thermal conductivity

Thermal conductivity of the four samples between 2 and 300 K is plotted in Fig. 8. The thermal conductivity of these Mm-filled skutterudites is significantly lower than that of their binary parent compounds $CoSb_3$ over the entire temperature range.[21] The estimated room temperature lattice thermal conductivities of these samples using the

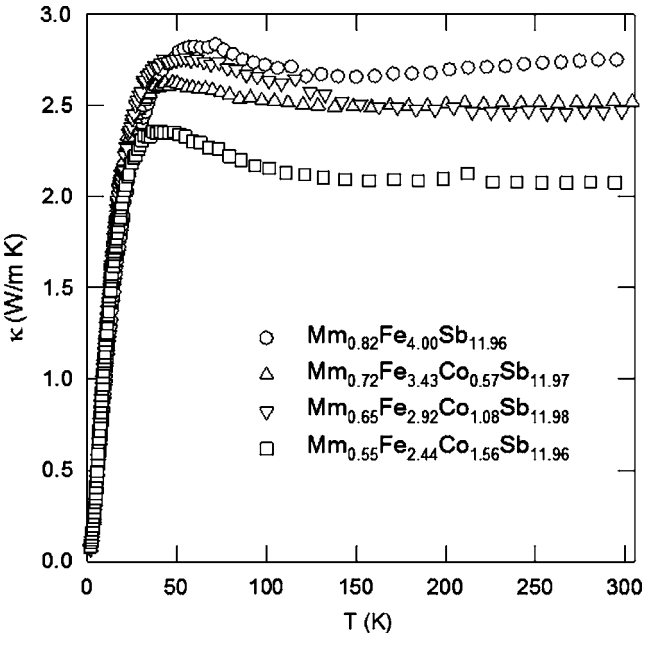

FIG. 8. Thermal conductivity vs temperature between 2 and 300 K for $Mm_yFe_{4-x}Co_xSb_{12}$.

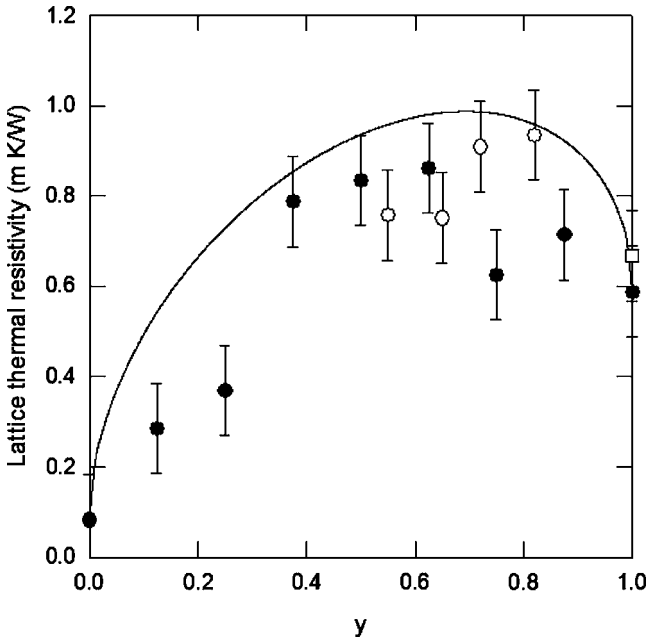

FIG. 9. Room temperature lattice thermal resistivity of $Ce_yFe_{4-x}Co_xSb_{12}$ (Ref. 10) (filled circles), $LaFe_4Sb_{12}$ (unfilled square) (Ref. 2), and $Mm_yFe_{4-x}Co_xSb_{12}$ (unfilled circles) vs y. Solid line represents the calculated thermal resistivity based on solid solution formation of fully filled and unfilled sublattices (Ref. 10).

Wiedemann-Franz law are between 1.0 and 1.3 W/m K, comparable to those reported for Ce- and La-filled skutterudites.[10,2] These low lattice thermal conductivity values are attributed to the rattling rare-earth atoms on the Mm sites, as evidenced by their large atomic displacement parameters, that interact with heat carrying lattice phonons, consistent with the large body of literature already developed on filled skutterudites. Figure 9 shows the room temperature lattice thermal resistivity of $Ce_yFe_{4-x}Co_xSb_{12}$,[10] $LaFe_4Sb_{12}$,[2] and $Mm_yFe_{4-x}Co_xSb_{12}$ versus y. Data for $Mm_yFe_{4-x}Co_xSb_{12}$ are not only comparable to those of $Ce_yFe_{4-x}Co_xSb_{12}$, but also follow the trend predicted by the model of Callaway and von Baeyer.[10] This substantiates that the lattice thermal conductivity of filled skutterudites is also strongly influenced by the static disorder of the occupied and unoccupied voids.

IV. SUMMARY AND CONCLUSIONS

We have studied the effect of Mm filling on the interstitial voids of skutterudites by measuring x-ray and neutron powder diffraction, electrical resistivity, thermopower, Hall effect, and thermal conductivity of a series of $Mm_yFe_{4-x}Co_xSb_{12}$ samples between 2 and 300 K. Mm filling causes larger expansion and unusual distortion of the $CoSb_3$ lattice compared with single-element-filled skutterudites. Our data reveal that rare-earth atoms on the Mm sites have larger atomic displacement parameters with much stronger temperature dependence than Fe/Co and Sb sites. Mm filling gives rise to both static and dynamic disorder at Mm sites of the crystal structure. While the filled and the unfilled voids give rise to static disorder, dynamic disorder is attributed to thermally induced rattling of rare-earth atoms around their equilibrium positions. The average rattling frequency of rare-earth atoms at Mm sites are comparable to those found in

single-rare-earth filled skutterudites. The electrical resistivity, thermopower, and thermal conductivity of Mm-filled skutterudites are similar to those Ce-filled skutterudites with comparable compositions, but do not reflect the unusual lattice distortion seen in the diffraction/structural results. The interaction between rattling rare-earth atoms with heat carrying lattice phonons results in low thermal conductivity, and high effective band masses lead to large power factors, which are reminiscent of Ce-filled skutterudites.

ACKNOWLEDGMENTS

J.Y. and G.P.M. want to thank Dr. Jan F. Herbst and Dr. Mark W. Verbrugge for continuous support and encouragement. The authors would like to thank R. A. Waldo and M. P. Balogh for assistance in EPMA and x-ray diffraction measurements. The work is in part supported by GM, by DOE under corporate agreement DE-FC26-04NT42278, by the Assistant Secretary for Energy Efficiency and Renewable Energy, Office of Transportation Technologies as part of the High Temperature Materials Laboratory User Program, and by the Waste Heat Recovery Program via the corporate agreement DE-FC26-04NT42278 at Oak Ridge National Laboratory managed by the UT-Battelle LLC, for the Department of Energy under contract DE-AC05000OR22725. Certain trade names and company products are identified in order to specify experimental procedures adequately. In no case does such identification imply recommendation or endorsement by the National Institute of Standards and Technology, nor does it imply that the products are necessarily the best available for the purpose.

[1]C. Uher, in *Recent Trends in Thermoelectric Materials Research I*, Semiconductors and Semimetals, Vol. 69, edited by T. M. Tritt (Academic, San Diego, 2000), p. 139, and references therein.
[2]B. C. Sales, in *Handbook on the Physics and Chemistry of Rare Earths*, edited by K. A. Gschneider, Jr., J.-C. G. Bünzli, and V. K. Pecharsky (Elsevier Science and Technology, Amsterdam, 2003), Vol. 33, and references therein.
[3]G. S. Nolas, D. T. Morelli, and T. M. Tritt, Annu. Rev. Mater. Sci. **29**, 89 (1999), and references therein.
[4]J. Yang and C. Caillat, MRS Bull. **31**, 224 (2006).
[5]D. Bérardan, C. Godart, E. Alleno, S. Berger, and E. Bauer, J. Alloys Compd. **351**, 18 (2003); D. Bérardan, E. Alleno, and C. Godart, J. Magn. Magn. Mater. **285**, 245 (2005); D. Bérardan, E. Alleno, C. Godart, M. Puyet, B. Lenoir, R. Lackner, E. Bauer, L. Girard, and D. Ravot, J. Appl. Phys. **98**, 033710 (2005).
[6]B. Bourgoin, D. Bérardan, E. Alleno, C. Godart, O. Rouleau, and E. Leroy, J. Alloys Compd. **399**, 47 (2005).
[7]B. H. Toby, J. Appl. Crystallogr. **34**, 210 (2001).
[8]A. C. Larson and R. B. Von Dreele, Los Alamos National Laboratory Report No. LAUR 86–748, 2000.
[9]V. F. Sears, Neutron News **3**, 26 (1992).
[10]G. P. Meisner, D. T. Morelli, S. Hu, J. Yang, and C. Uher, Phys. Rev. Lett. **80**, 3551 (1998).
[11]J. Yang, G. P. Meisner, D. T. Morelli, and C. Uher, Phys. Rev. B **63**, 014410 (2000).
[12]D. J. Braun and W. Jeitschko, J. Less-Common Met. **72**, 147 (1980).
[13]B. C. Chakoumakos and B. C. Sales, J. Alloys Compd. **407**, 87 (2006).
[14]J. W. Kaiser and W. Jeitshko, J. Alloys Compd. **291**, 66 (1999).
[15]B. C. Sales, B. C. Chakoumakos, and D. Mandrus, Phys. Rev. B **61**, 2475 (2000).
[16]V. Keppens, D. Mandrus, B. C. Sales, B. C. Chakoumakos, P. Dai, R. Coldea, M. B. Maple, D. A. Gajewski, E. J. Freeman, and S. Bennington, Nature (London) **395**, 876 (1998).
[17]G. L. Long, R. P. Hermann, F. Grandjean, E. E. Alp, W. Sturhahn, C. E. Johnson, D. E. Brown, O. Leupold, and R. Rüffer, Phys. Rev. B **71**, 140302(R) (2005).
[18]B. C. Sales, B. C. Chakoumakos, and D. Mandrus, in *Recent Trends in Thermoelectric Materials Research II, Semiconductors and Semimetals*, edited by T. M. Tritt (Academic, San Diego, 2000), Vol. 70, p. 1.
[19]J. Yang, D. T. Morelli, G. P. Meisner, W. Chen, J. S. Dyck, and C. Uher, Phys. Rev. B **67**, 165207 (2003).
[20]G. A. Slack and M. A. Hussain, J. Appl. Phys. **70**, 2694 (1991).
[21]J. Yang, D. T. Morelli, G. P. Meisner, W. Chen, J. S. Dyck, and C. Uher, Phys. Rev. B **65**, 095114 (2002).
[22]B. C. Sales, D. Mandrus, B. C. Chakoumakos, V. Keppens, and J. R. Thompson, Phys. Rev. B **56**, 15081 (1997).
[23]R. Viennois, S. Charar, D. Ravot, P. Haen, A. Mauger, A. Bentien, S. Paschen, and F. Steglich, Eur. Phys. J. B **46**, 257 (2005).
[24]K. Magishi, Y. Nakai, K. Ishida, H. Sugawara, I. Mori, T. Saito, and K. Koyama, J. Phys. Soc. Jpn. **75**, 023701 (2006).